

Montclair State University Montclair State University Digital Commons

Department of Earth and Environmental Studies
Faculty Scholarship and Creative Works

Department of Earth and Environmental Studies

10-15-2011

Linkages between East Antarctic Ice Sheet Extent and Southern Ocean Temperatures Based on a Pliocene High-resolution Record of Ice-rafted Debris off Prydz Bay, East Antarctica

Sandra Passchier

Montclair State University, passchiers@montclair.edu

Follow this and additional works at: <https://digitalcommons.montclair.edu/earth-environ-studies-facpubs>

 Part of the [Geology Commons](#), and the [Glaciology Commons](#)

MSU Digital Commons Citation

Passchier, Sandra, "Linkages between East Antarctic Ice Sheet Extent and Southern Ocean Temperatures Based on a Pliocene High-resolution Record of Ice-rafted Debris off Prydz Bay, East Antarctica" (2011). *Department of Earth and Environmental Studies Faculty Scholarship and Creative Works*. 38.

<https://digitalcommons.montclair.edu/earth-environ-studies-facpubs/38>

Published Citation

Passchier, S. (2011). Linkages between East Antarctic Ice Sheet extent and Southern Ocean temperatures based on a Pliocene high-resolution record of ice-rafted debris off Prydz Bay, East Antarctica. *Paleoceanography*, 26. doi:10.1029/2010PA002061

Linkages between East Antarctic Ice Sheet extent and Southern Ocean temperatures based on a Pliocene high-resolution record of ice-rafted debris off Prydz Bay, East Antarctica

S. Passchier¹

Received 28 September 2010; revised 2 June 2011; accepted 12 July 2011; published 15 October 2011.

[1] Ice-rafted debris mass accumulation rates (IRD MAR) at a drill site on the Antarctic continental margin are investigated to evaluate the linkages between East Antarctic Ice Sheet extent and Southern Ocean temperatures in the early to mid-Pliocene. ODP Site 1165 is within 400 km of the Antarctic coastline and in the direct pathway of icebergs released by the Amery Ice Shelf. The Amery Ice Shelf is the largest ice shelf in East Antarctica and it buttresses the Lambert Glacier drainage system, which accounts for 14% of the outflow from the East Antarctic Ice Sheet. IRD MAR were low during peak Southern Ocean warming in the early Pliocene. After a brief precursor, a tenfold increase in IRD MAR at 3.3 Ma marks the termination of the early Pliocene ice sheet minimum, coincident with the M2 glacial. For the mid-Pliocene, a strong correlation exists between the high-amplitude signal in the LR04 benthic stack and IRD MAR, suggesting linkages between East Antarctic ice extent, global ice volume and deep-water temperatures. The IRD record at Site 1165 provides evidence of greater sensitivity of the Lambert Glacier-Amery Ice Shelf system to Southern Ocean warming than is currently predicted by ice sheet models, which may relate to uncertainties in the understanding of ocean heat uptake, poleward heat transport and ice sheet-ocean interactions.

Citation: Passchier, S. (2011), Linkages between East Antarctic Ice Sheet extent and Southern Ocean temperatures based on a Pliocene high-resolution record of ice-rafted debris off Prydz Bay, East Antarctica, *Paleoceanography*, 26, PA4204, doi:10.1029/2010PA002061.

1. Introduction

[2] The Pliocene was the last epoch wherein the atmospheric pCO₂ was similar to today's partial pressure and atmospheric global temperatures were higher than the modern [Hönisch *et al.*, 2009; Pagani *et al.*, 2010; Seki *et al.*, 2010]. In comparison with pre-industrial conditions, the world was 4°C warmer with pCO₂ estimated at 90–125 ppm higher at ~4–4.5 Ma [Brierley *et al.*, 2009; Pagani *et al.*, 2010; Seki *et al.*, 2010]. How the Antarctic Ice Sheets responded to perturbations in the climate system under these conditions is a major question with relevance in the light of climate change predictions [Jansen *et al.*, 2007]. Ninety percent of the ice discharge occurs through ice streams and large outlet glaciers and the vulnerability of these to climate change is uncertain [Bamber *et al.*, 2000]. Increased surface melting, ice shelf collapse, and changing basal ice conditions may result in nonlinear responses of ice sheets to warming through accelerated flow of outlet glaciers and

additional discharge of ice [Zwally *et al.*, 2002; Pritchard and Vaughan, 2007]. Although there is mounting evidence that the West Antarctic Ice Sheet was unstable in the Pliocene [Naish *et al.*, 2009; Pollard and DeConto, 2009], the stability of the larger East Antarctic Ice Sheet (EAIS) is considerably debated [e.g., Harwood and Webb, 1998; Sugden and Denton, 2004; Haywood *et al.*, 2009a]. Although complete collapse of the EAIS is very unlikely from a modeling perspective, East Antarctic ice volume reductions of 2–3 m global sea level equivalents have been predicted [Hill *et al.*, 2007; Pollard and DeConto, 2009]. The timing and spatial pattern of the retreat, however, is poorly constrained by data sets from the Antarctic continental margin, because current records are not documenting glacial dynamics with sufficient resolution and chronology. Here I present a medium to high resolution record of the ice rafting history off Prydz Bay near the outlet of the Lambert Glacier-Amery Ice Shelf system, as it reflects on the ice-dynamical responses of a major drainage pathway of the EAIS [Rignot and Thomas, 2002] (Figure 1).

[3] The Pliocene is characterized as a period of higher global surface temperatures [Dowsett *et al.*, 1996; Thompson and Fleming, 1996], with sea level locally rising to between 5 and 35 m above the present level [Dowsett and

¹Department of Earth and Environmental Studies, Montclair State University, Upper Montclair, New Jersey, USA.

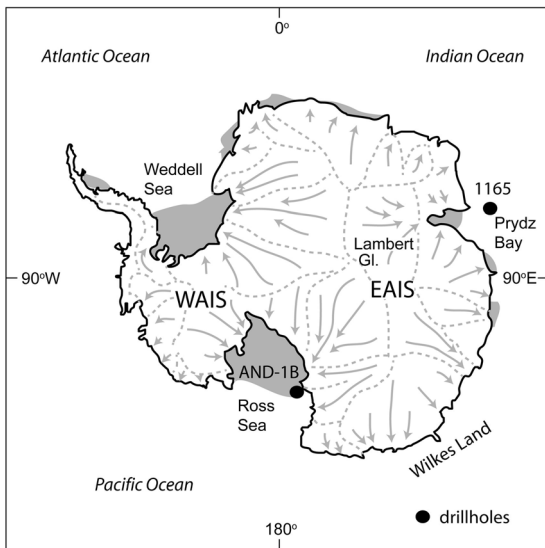


Figure 1. Ice sheet flow patterns and location of Site 1165 on the East Antarctic Continental Margin.

Cronin, 1990; Krantz, 1991; Miller *et al.*, 2005; Naish and Wilson, 2009; Naish *et al.*, 2009]. Early mid Pliocene pCO_2 fluctuated between ~ 350 and 450 ppm, near the modern values and those predicted for the end of this century, with a decline to persistent lower values in the late Pliocene [Hönisch *et al.*, 2009; Pagani *et al.*, 2010; Seki *et al.*, 2010]. The Pliocene, therefore, is an excellent time interval to study the long-term stability of ice sheets in a world comparable to the present and the near future. Tectonically and oceanographically the Earth was similar to today, because the Panama Seaway had shoaled enough to block exchange of water between the Atlantic and the Pacific Ocean and the Gulf Stream began feeding warm saline waters into the North Atlantic Ocean [Billups *et al.*, 1998; Haug *et al.*, 2001; Steph *et al.*, 2006]. Recent climate modeling studies suggest that the early mid Pliocene prior to the onset of Northern Hemisphere glaciation potentially experienced a constant El Niño state [Wara *et al.*, 2005; Brierley *et al.*, 2009], but the cause of the Pliocene warming and the role of the El Niño-Southern Oscillation are debated [Haywood *et al.*, 2009b; Brierley *et al.*, 2009]. Both models and data, however, suggest that warmth was unevenly distributed across the globe with the greatest degree of warming in the high latitudes [Tedford and Harington, 2003; Ashworth and Thompson, 2003; Haywood *et al.*, 2009b; Ballantyne *et al.*, 2010].

[4] Significant warming at high latitudes potentially impacted the extent and dynamics of the Pliocene ice sheets and associated sea ice and sea level effects. Diatomaceous sediments and associated facies indicating early Pliocene ice retreat away from the Antarctic coast near Prydz Bay between 4.9 and 4.1 Ma have been known for some time [Pickard *et al.*, 1988; McMinn and Harwood, 1995; Whitehead *et al.*, 2004]. Although showing important and unique evidence of glacial extent, the fragmentary nature and poor chronology of these outcrops inhibited direct correlation to global climate proxies and have caused considerable debate [Harwood and Webb, 1998; Hambrey and McKelvey, 2000; Sugden and Denton, 2004]. A dynamic

versus stable ice sheet controversy developed, first centered on the age of the Sirius Group in the Transantarctic Mountains, which consists of remnants of glacial sequences deposited by temperate or polythermal glaciers. According to the dynamic ice sheet hypothesis, diatom assemblages incorporated in the Sirius Group record periods when the Wilkes and Aurora subglacial basins (Figure 2) were ice-free and became inundated by the sea several times until as recent as the early Pliocene [Harwood, 1986; Harwood and Webb, 1998]. According to proponents of the stable ice-sheet hypothesis, however, numeric ages of >14 Ma for in situ, unweathered, ash deposits from the higher elevated regions of the Transantarctic Mountains [Marchant *et al.*, 1993] constrain the more temperate climatic and ice sheet conditions indicated by the Sirius Group to the middle Miocene or older. These authors argue that Antarctica has been covered by a stable polar ice sheet under frigid polar conditions persistently since this time. Because of the apparent discrepancy, the origin and transport paths of the diatoms in the Sirius Group have been disputed [Gersonde *et al.*, 1997; Stroeven *et al.*, 1998] and the controversy around the age of the Sirius Group and the minimum size of the EAIS in the early Pliocene remains unresolved.

[5] Significant progress, however, has been made in reconstructing early mid Pliocene Antarctic paleoenvironments and sea surface temperatures from drillcores coupled with climate modeling. In studies of DSDP cores and ODP Sites 748 and 751 (Figure 3) five intervals of Pliocene warming in the Southern Ocean were recognized: 4.5, 4.3, 3.6, 3.1 and 3.0 Ma, based on the distribution of *Dictyochoa* silicoflagellates and calcareous nannoplankton, which occur north of the Antarctic Polar Front today [Ciesielski and Weaver, 1974; Bohaty and Harwood, 1998]. While the presence of calcareous nannoplankton in the two mid-Pliocene intervals (3.1, 3.0 Ma) represents moderate warming to $\sim 3^\circ C$ above present, with diatoms indicating reduced sea ice coverage at Sites 1166 and 1165 [Whitehead *et al.*, 2005], the early Pliocene intervals at 4.5, 4.3, and 3.6 Ma also

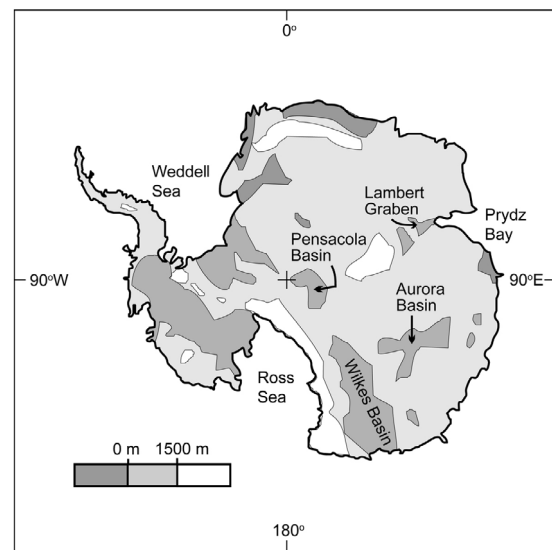


Figure 2. Simplified bed topography beneath the Antarctic Ice Sheet (after Lythe *et al.* [2001]).

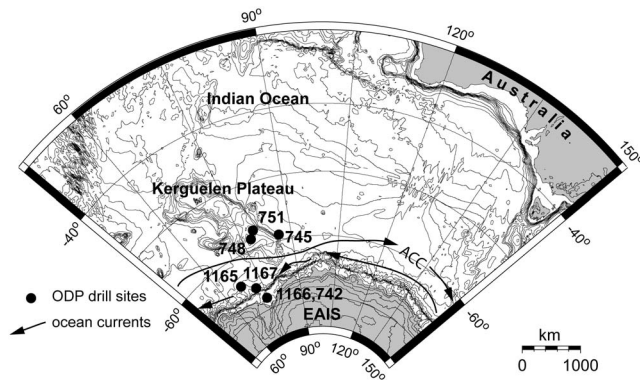


Figure 3. Location of Ocean Drilling Program (ODP) drill sites in the Prydz Bay sector of the Southern Ocean. ACC: Antarctic Circumpolar Current.

contain the silicoflagellate *Dictyocha* and likely represent a greater degree of warming. Other estimates based on silicoflagellate and diatom assemblages in lower Pliocene strata of Site 1165 indicate that SST may have been ~ 4 to 5.5°C higher than present at 4.9–4.6, 4.3, and 3.6 Ma [Whitehead and Bohaty, 2003; Escutia et al., 2009]. Open marine conditions between 4.9 and 3.6 are also recognized in two beds with in situ diatom floras from Site 739 in Prydz Bay [Baldauf and Barron, 1991]. Early Pliocene warming and ice at its minimum extent is also evident in the record of the AND-1B core (Figure 1): on the continental shelf of the Ross Sea, open marine conditions with elevated sea surface temperatures were recognized at 4.9–4.8 Ma, 4.7 Ma and 4.5 Ma, and no evidence of grounded ice was found between 4.6 and 3.4 Ma [Naish et al., 2009]. These studies provide a consistent pattern of Southern Ocean warming in the early and mid-Pliocene with several episodes of peak warming between 4.9 and 3.6 Ma.

[6] Warmer sea surface temperatures in the Pliocene likely resulted in increased melting of marine termini and reduced sea ice conditions and it is suggested that the West Antarctic Ice Sheet collapsed periodically [Naish et al., 2009]. In previous IRD studies in the Southern Ocean periods of high IRD mass accumulation rates are found at 4.9–4.5 Ma, with distinct peaks at 4.9 and 4.6 Ma [Pudsey, 1991; Allen and Warnke, 1991; Breza, 1992; Murphy et al., 2002; Joseph et al., 2002] (timescales converted to those of Gradstein et al. [2004]). In contrast, generally low IRD mass accumulation rates occur at 4.5–3.3 Ma with an abrupt increase in IRD after 3.3 Ma [Breza, 1992]. The resolution of these studies, however, is too low to provide detailed comparison to global proxy records of paleoclimate and ice dynamics or model results. Most of these studies were also further offshore and were probably recording ice-rafting from both the East and the West Antarctic Ice Sheet.

[7] In continental margin drill sites, IRD mass accumulation rates more likely represent the local IRD production as is confirmed by geochemical provenance studies of IRD from the Antarctic continental margin [Roy et al., 2007; Cowan et al., 2008; Williams et al., 2010]. Here, ice-rafted debris mass accumulation rates (IRD MAR) of Site 1165 on the continental rise off Prydz Bay are interpreted in the context of previous studies on glacial continental shelf and slope successions [Rebesco et al., 2006; O'Brien et al.,

2007; Volpi et al., 2009]. According to the Antarctic Iceberg Tracking Database (1978–2009) (available at <http://www.scp.byu.edu/data/iceberg/database1.html>) today most large icebergs released from East Antarctica do not travel further offshore than a few hundreds of kilometers. Near Prydz Bay, the majority of icebergs is carried westward with the continental slope current, but clusters of icebergs originating from East Antarctic ice shelves also occur at 64 and 62°S, suggesting a preferred drift pattern further north where it joins the Antarctic Circumpolar Current (ACC) (Figure 4) [Young et al., 1998]. Because of its position in the Antarctic Divergence and its distant location from West Antarctic drainage basins, such as the Weddell Sea and the Ross Sea, Site 1165 is not likely to receive IRD originating from West Antarctica. The advantage of continental margin records, such as Site 1165, is further that sedimentation rates are higher, providing for higher resolution records, less impacted by bioturbation and amalgamation of IRD layers through sediment loading and vertical mixing.

[8] The Prydz Bay area is the depocenter for sediment supplied by the Lambert Glacier system, which, at present, drains about 14% of the total outflow from the EAIS (Figure 1) [Rignot and Thomas, 2002]. The Lambert Glacier is buttressed by the Amery Ice Shelf, the largest ice shelf in East Antarctica, which is potentially susceptible to rapid retreat because of the northerly position of its calving front at 69°S. The Lambert Glacier system is currently only experiencing insignificant mass loss [Rignot et al., 2008; Pritchard et al., 2009]. However, in recent years the ice shelf has seen an increase in the areal extent of surface meltwater streams, and two areas at its base are composed of ~ 100 m thick porous accreted marine ice, which is highly susceptible to melting by infiltration of warmer seawater [Fricker et al., 2001, 2009]. Knowing how the ice shelf responded to previous episodes of warming, notably the Pliocene warm events, is of great interest and importance, because of uncertainties in predictions of meridional heat transport under a warming climate [e.g., Brierley et al., 2009].

[9] The Lambert Glacier is currently grounded about 0.6 km below sea level, headward of a deep structural basin, the Lambert Graben. The Amery Ice Shelf covers the Lambert Graben which is sloping landward from its outlet in

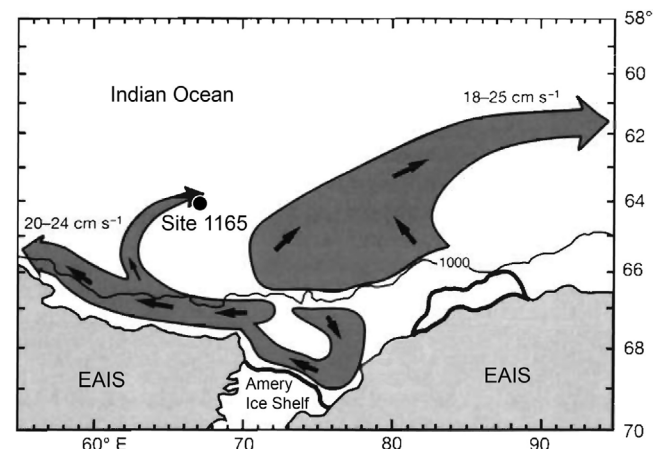


Figure 4. Flow patterns in Prydz Bay derived from iceberg track records. Adapted from work by Hosie and Cochran [1994, Figure 3].

Table 1. Age Tie Points for the Early Mid Pliocene at Site 1165^a

Depth (mbsf ^b)	Age (Ma)	LSR ^c (cm/kyr)
14.99	1.77	
19.23	3.032	0.56
20.91	3.116	2.00
25.96	3.207	5.54
30.76	3.33	3.90
36.46	3.596	2.14
42.06	4.187	0.94
46.96	4.799	0.80
49.12	4.997	1.09
54.56	5.235	2.28

^aAges are based on work by *Florindo et al.* [2003] and *Villa et al.* [2008].

^bMeters below seafloor.

^cLinear Sedimentation Rate.

Prydz Bay to depths larger than 1.5 km within 100 km of the present grounding line [*Whitehead et al.*, 2006]. One of the objectives of Ocean Drilling Program Leg 188 was to reconstruct Neogene variations in the extent of the Lambert Glacier-Amery Ice Shelf system. The morphology of the shelf in Prydz Bay shows evidence of excavation of a channel and the development of a trough-mouth fan through extreme advances of the ice sheet [*O'Brien et al.*, 2007]. Ice-proximal strata drilled at Sites 1166 and 1167 (Figure 3) carry valuable direct evidence of glaciation, but with poor coverage of the warm Pliocene and multiple hiatuses [*Passchier et al.*, 2003; *O'Brien et al.*, 2007]. In contrast, Site 1165 (64° 22.77'S, 67° 13.14'E), which was drilled at a water depth of 3538 mbsf (meters below seafloor) in a sediment drift on the continental rise (Figure 3), yielded a relatively complete early to mid-Pliocene section.

2. Materials and Methods

[10] A total of 148 samples between 15.36 and 54.17 mbsf were analyzed from Hole 1165B to provide a high resolution record of terrigenous particle size and IRD MAR for the Pliocene of Site 1165. Sediments in this interval of core are characterized as three facies [*Shipboard Scientific Party*, 2001]. The core interval down to ~23 mbsf consists of interbedded structureless yellowish gray to brown diatom clay and diatom ooze. Below ~23 mbsf interbedded 2–5 m thick units of greenish gray and dark grayish brown diatom-bearing silty clay are present. The dark grayish brown units are laminated between ~25 and ~33 mbsf.

[11] The samples were pretreated with 30% H₂O₂, 10% HCl, and 0.2 M NaOH solution, to remove biogenic components and to preserve only the terrigenous silicate fraction [*Konert and Vandenberghe*, 1997]. Samples were dispersed by heating with sodium pyrophosphate. Grain-size distributions were measured on a Malvern Mastersizer 2000 laser particle sizer with a size range of 0.02–2000 μm with instrument settings following the recommendations of *Sperazza et al.* [2004]. IRD MAR was calculated from the sand percentage of the terrigenous fraction according to the methodology of *Krissek* [1995]. Corrections for the presence of biogenic carbonate were made using the percentage carbonate reported in shipboard data [*Shipboard Scientific Party*, 2001]. Biogenic silica content was estimated based on the relationship between biogenic silica and green-gray

ratio of sediments found by *Rebesco* [2003] and as applied by *Grütner et al.* [2005]. IRD MAR was calculated according to:

$$IRD\ MAR = \% IRD \times TERR \times DBD \times LSR$$

Where % IRD = vol. % > 125 micron of the laser particle size measurements, *TERR* = the terrigenous fraction defined as (1-biogenic silica fraction-carbonate fraction), *DBD* = dry bulk density derived from shipboard measurements [*Shipboard Scientific Party*, 2001], and *LSR* = linear sedimentation rate calculated from the age model.

[12] The age model applied here is that of *Florindo et al.* [2003] with modifications as recommended by *Villa et al.* [2008]. The recovery in the studied interval of core is >90% and ten age tie points are used to constrain the chronology (Table 1). Age tie points reflect those reversals for which the stratigraphic position is well constrained, taken into account short intervals of no recovery, core breaks, and biostratigraphic control [*Florindo et al.*, 2003; *Warnke et al.*, 2004]. All ages are converted to the *Gradstein et al.* [2004] timescale. According to these age models the early mid Pliocene interval between 54.56 and ~17 mbsf (5.2 to 3.0 Ma) is relatively intact, whereas the late Pliocene-early Pleistocene interval between ~17 and 15 mbsf (3.0–1.8 Ma) comprises a condensed section with several potential hiatuses [*Florindo et al.*, 2003; *Villa et al.*, 2008].

[13] In contrast to conventional methods, bulk particle size analysis provides an opportunity to separate coarse-grained current lags from “real” peaks in IRD abundance through an assessment of the sorting [*Folk and Ward*, 1957] in the fine fraction. Because this sorting parameter is derived from the terrigenous particle size distribution and does not require a correction for the presence of biogenic components or sedimentation rates, it serves as an independent control on the reliability of the IRD MAR. If a peak in the IRD MAR coincides with a well-sorted sand fraction, it is evident that the peak is the result of a high sand percentage caused by winnowing of fine-grained sediments by currents, rather than high IRD delivery. Such winnowed sand peaks have been identified previously where condensed intervals were located through chronostratigraphic methods [*Murphy et al.*, 2002], but might go undetected in intervals of core where age tie points are fewer.

3. Results

[14] In general, peaks in IRD MAR coincide with poorly sorted fine sediment fractions (<125 μm), suggesting that current scouring was not a major factor in the upper 54 mbsf of Site 1165 (Figure 5). Potential hiatuses were identified through the age model between ~17 and 15 mbsf [*Florindo et al.*, 2003; *Villa et al.*, 2008], but these did not result in spurious IRD MAR peaks (Figure 5).

[15] A dramatic change in terrigenous grain-size and clay mineralogy at ~33 mbsf in the Pliocene section of Site 1165 subdivides it into two intervals with significantly different sedimentological properties [*Warnke et al.*, 2004]. The interval between ~54 and 33 mbsf represents relatively silt-rich sediments with 2–5 m scale fluctuations in terrigenous grain-size (Figure 5). These fluctuations do not coincide

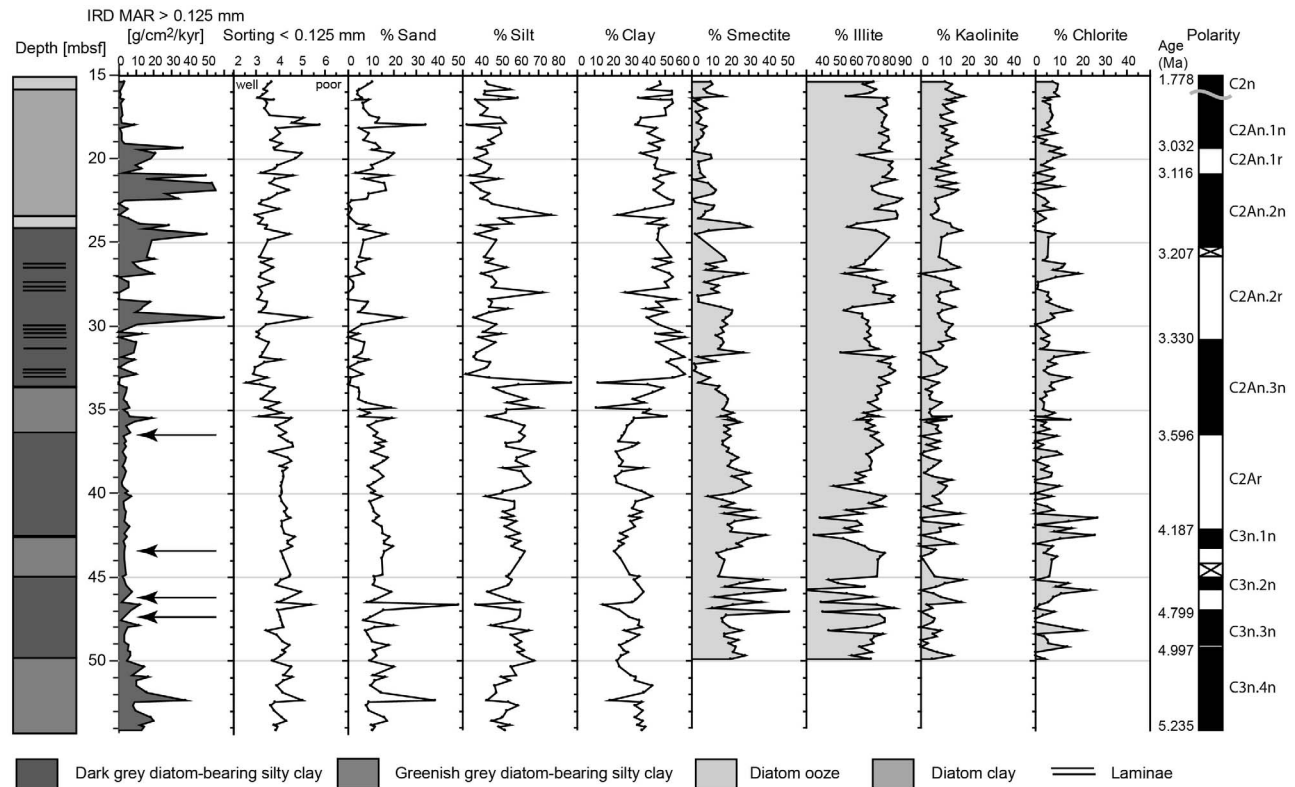


Figure 5. Depth distribution of ice rafted debris mass accumulation rates (IRD MAR), terrigenous silt and clay percentage, and clay mineral abundance at Site 1165. Arrows indicate positions of intervals recording sea surface temperatures 4–5.5°C higher than present [Whitehead and Bohaty, 2003; Escutia *et al.*, 2009]. Clay mineralogy from Junttila *et al.* [2005]. Magnetostratigraphy after Florindo *et al.* [2003] and Villa *et al.* [2008].

with facies transitions; the average particle size results do not show a significant difference between the structureless greenish gray and dark gray diatom-bearing silty clays. Some small peaks in IRD MAR occur in the lower half of the interval and are associated with poor sorting of the fraction < 125 μm . A dramatic change in terrigenous grain-size parameters is obvious at ~35–33 mbsf and the sediments above this interval have higher terrigenous clay percentages followed by a tenfold increase in IRD MAR at ~30 mbsf (Figure 5). Laminated interbeds occur at 33–26 mbsf. Some occur immediately below IRD MAR maxima, are moderately sorted, and generally contain around 45% silt. Some very silt-rich beds with up to 87% silt occur at ~33, 28 and 23 mbsf. Toward the top of the interval the sorting of the fraction < 125 μm decreases. This trend abruptly terminates at ~17 mbsf.

[16] Clay mineral data from Site 1165 [Junttila *et al.*, 2005] indicate a predominance of smectite and illite in the clay mineral assemblages with subordinate kaolinite and chlorite (Figure 5). Terrigenous clay percentage anti-correlates with smectite abundance and correlates with illite. Minima in clay % in the terrigenous fraction locally coincide with large abundances of *Dictyocha* silicoflagellates (Figure 5) at 35.54–37.62 mbsf, 43.57–43.77, 46.17 and 47.07 mbsf [Whitehead and Bohaty, 2003; Escutia *et al.*, 2009]. The large peaks in IRD MAR between ~30 and 17 mbsf coin-

cide with smectite peaks and low or declining proportions of illite.

3.1. Sedimentological Interpretation

[17] Sediments are delivered to glaciated continental margins mainly through glacial transport and meltwater streams and are redistributed by eolian and oceanographic processes. In the marine environment, besides particle size data, clay minerals derived from the <2 μm fraction of the sediments are useful in paleoenvironmental interpretations, because this fraction is carried as suspended load in far-traveled bottom and surface currents [Hillenbrand and Ehrmann, 2005]. Studies of Neogene strata in the Lambert Graben suggest that the clay mineralogy of the sediments there is primarily controlled by provenance [Ehrmann *et al.*, 2003]. Here I use the terrigenous particle size data in conjunction with previously published clay mineral data [Junttila *et al.*, 2005] to construct a sedimentation model for the early and mid-Pliocene of Site 1165.

[18] The interval between ~54 and 33 mbsf is characterized by 2–5 m-scale cyclical, gradational, changes in particle size and clay mineralogy with an anti-correlation of terrigenous clay and smectite percentages (Figure 5). The repetitive changes in color, particle size, and mineralogical composition are typical of high-latitude deep-water contourites from the Antarctic margin [Ehrmann and Grobe, 1991; Pudsey, 2000; Lucchi *et al.*, 2002]. Known sources

of smectite are present to the north of Site 1165 in the volcanic rocks of the Kerguelen Plateau, in the exposed rift flank of the Lambert Graben [Hultsch *et al.*, 2008], and the upper Eocene strata within the Prydz Bay continental shelf [Forsberg *et al.*, 2008]. The primary clay mineral in the Eocene strata in Prydz Bay, however, is kaolinite. Considering the paucity of kaolinite in the sediment supply in the ~54–33 mbsf core interval, a source of smectite by erosion of the shelf during glacial advances is not very likely. The poor stratification and low sedimentation rates (Table 1) further indicate that fine-grained sediment supply was mainly originating through suspension settling from turbid surface plumes or laterally from slow-flowing bottom currents.

[19] In contrast to the ~54–30 mbsf core interval, the terrigenous fraction of sediments between ~33 and 17 mbsf contains a large proportion of clay-sized particulates (Figure 5). Further, a tenfold increase in IRD MAR occurs at ~30 mbsf, suggesting an increase in deposition from icebergs at Site 1165. The predominant clay mineral in this interval is illite [Junttila *et al.*, 2005]. Illite is a very stable clay mineral in the marine environment and could originate from physical erosion of crystalline rocks [Ehrmann *et al.*, 2003] or clay-rich marine sediments to produce tills with >50% illite in the clay fraction as observed beneath a modern ice stream [Tulaczyk *et al.*, 1998]. Fjoridal systems flanked by temperate tidewater fronts may act as significant sediment traps for illite-rich glacially weathered sediments [Powell and Molnia, 1989; Dowdeswell *et al.*, 1998; Ó Cofaigh *et al.*, 2001], sediment which may become reworked and redeposited upon glacial advance. The increase in clay-sized material may hence be indicative of a grounding-line advance into the Lambert Graben. Alternatively, the increase in clay content could signal a decrease in bottom current speeds, associated with a northward directed shift in the ACC. Settling of clays may further have been augmented by enhanced flocculation in response to an increase in salinity of shelf-derived bottom waters.

[20] Between ~33 and 26 mbsf, the dark gray diatom-bearing clays locally contain sets of silt laminae with a fine-grained tail, which occur at the base of intervals with high IRD MAR. No obvious graded beds or current ripples are present in the laminated intervals, and sedimentation rates are high. A similar combination of facies has been found associated with Heinrich events on the North Atlantic continental margins near outlets of large paleo ice streams [Hesse *et al.*, 1997; Lekens *et al.*, 2005], albeit with different age relationships. In accordance with existing sedimentation models for sediment drifts on the Antarctic continental rise [Pudsey, 2000; Lucchi *et al.*, 2002], the sediments could originate from meltwater plumes or low-density turbidity currents, released from a Lambert ice stream grounded at the shelf edge. Alternatively the sediments could be related to dense, saline, currents originating from brine formation on the Prydz Bay continental shelf. The increase in sedimentation rates, paucity of sand, and a lack of bioturbation of these laminated beds suggests that deposition was relatively fast and continuous, which is inconsistent with a contour current origin [Lucchi *et al.*, 2002].

3.2. Interpretation of the IRD MAR

[21] Fast-flowing ice streams and outlet glaciers are the primary sources of IRD in the marine environment [Ó Cofaigh *et al.*, 2001; Death *et al.*, 2006]. Glacial erosion and entrainment of basal debris takes place in the marginal area of a glacier or ice stream where the driving stress increases to overcome the strength of the subglacial bed. Where outlet glaciers extend through glacial valleys with steep bedrock walls, englacial or supraglacial debris will contribute to the sediment load of icebergs. When the marginal area is warm-based and overlies a rock bed, abundant sand and silt-sized rock flour is produced by glacial comminution. The comminution of large rock fragments to silt-sized particles, however, is reduced beneath both cold-based and polythermal glaciers [Hambrey *et al.*, 1999] and when ice streams overlie a soft sediment bed of clay-rich sediments [Tulaczyk *et al.*, 1998]. Cold ice margins are associated with ice shelves in the marine environment and, under present-day conditions, Antarctic ice shelves become unstable once surface temperatures rise to values between -9 and -5°C [Cook *et al.*, 2005]. In comparison to temperate tidewater glaciers, icebergs generated by steady state calving of ice shelves are typically larger and occur in clusters [Young *et al.*, 1998]. The debris deposited by retreating ice shelves contains significantly more sand and gravel by volume [Evans and Pudsey, 2002], is typically of supraglacial origin, with greatest depositional rates occurring near the calving line of an ice shelf [Domack and Harris, 1998]. Thus, although ice shelves generate less basal debris, more of the debris is sand-sized due to a lack of comminution under polar glacier margins.

[22] Factors that can influence the debris content of glaciers and icebergs are: basal thermal regime, subglacial hydrology, and the topography and the composition of the subglacial bed. Modeling studies suggest that deposition of basal debris is the greatest on the shelf and trough mouth fans of large temperate outlet glaciers within a few hundreds of kilometers of the grounding line, but englacial debris may be carried further [Death *et al.*, 2006]. Ice front geometry, glacier flow speed and calving rate further influence iceberg production and size, whereas coastal morphology, sea-ice extent, water temperature, and ocean currents have a strong influence on iceberg survival, residence time, and the spatial distribution of icebergs.

[23] The primary factors controlling the IRD MAR record at Site 1165 are the position of the Antarctic Circumpolar Current (ACC), ice extent, calving rate, and sea surface temperature, which are strongly connected. In one model simulation, the growth of a large continental ice sheet grounded on the shelf during glacials coincides with a decrease in austral winter temperatures in excess of 10°C over a large proportion of the Southern Ocean [DeConto *et al.*, 2007]. The implication is that because Site 1165 is proximal to the site of iceberg production, ice extent and SST are coupled. A scenario where icebergs are produced from extensive grounded ice in warmer waters, resulting in release of most IRD nearshore before reaching Site 1165, is therefore unlikely. Although basal meltout from floating termini might result in the release of most basal debris prior to calving, icebergs produced from rock-walled outlet glaciers,

such as the Lambert Glacier, contain significant sand-sized englacial or supraglacial debris [Hambrey and McKelvey, 2000], which will be carried to Site 1165 under the low SST associated with marine-grounded margins [DeConto *et al.*, 2007].

[24] Provenance studies of Neogene IRD maxima in Site 1165 do not reflect a large role for changes in surface currents [Williams *et al.*, 2010]. Site 1165 is less than 400 km from the East Antarctic coastline and landward of the present position of the ACC (~62°S) [Bindoff *et al.*, 2000] (Figure 3). Provenance studies of IRD maxima in Site 1165 suggest that more than 50% of the material is locally derived and shows a combined local and easterly source [Williams *et al.*, 2010], which is consistent with the present surface currents (Figure 3). Therefore, during times of maximum ice conditions in East Antarctica, it is likely that Site 1165 saw an increase in IRD deposition due to the combined effects of IRD production from calving marine-based ice margins, iceberg survival due to low SST, and a northerly position of the ACC. A retreat of the ice sheet could have resulted in a southward shift in the position of the ACC due to a reduction in the meridional pressure gradient. Such a shift is not visible in the IRD provenance data [Williams *et al.*, 2010], but it should be noted that the coastline directly west of Prydz Bay lacks large marine-grounded ice streams or outlet glaciers [Rignot and Thomas, 2002]. A southward shift in the position of the ACC could have generated a decrease in the supply of IRD rather than IRD MAR maxima with a westerly source.

[25] The decrease toward low MAR of coarse-grained sand-sized IRD at ~54–33 mbsf therefore suggests that the ice sheet receded to within the Lambert Graben, possibly terminating on land during interglacials, supporting warmer SST and a southward migration of the ACC. The contourite sedimentation model for the sediments between ~54 and 33 mbsf supports this scenario. The tenfold increase in IRD MAR at ~33 mbsf is best explained as ice advance, cooling of SST and a northward migration of the ACC. This interpretation is consistent with the clay provenance and sedimentation model indicating downslope transport and the increased sedimentation rates (Table 1).

4. Early Pliocene Ice Dynamics

[26] Although there is general consensus that the Southern Ocean experienced higher temperatures between 5.0 and 3.7 Ma [e.g., Ciesielski and Weaver, 1974; Burckle *et al.*, 1996; Bohaty and Harwood, 1998; Escutia *et al.*, 2009], considerable debate exists about its effect on the dynamics of the EAIS. Several Southern Ocean records have high concentrations of IRD between 5.3 and 3.4 Ma [e.g., Warnke *et al.*, 1992], indicating substantial iceberg production from marine-based glaciers. However, these records are far offshore and may not record East Antarctic ice sheet dynamics. Glacial unconformities and diamictites on the Prydz Bay continental shelf are indicative of ice sheet advance between the late Miocene and mid-Pliocene. However, the chronology of these glacial erosion events is poor and a consensus is lacking [Bart, 2001; Passchier *et al.*, 2003; O'Brien *et al.*, 2007; Volpi *et al.*, 2009].

[27] The chronology of Site 1165 is constrained by ten age tie points (Table 1) and the IRD MAR record and

sedimentation model both indicate that ice extent was most likely decreased between 4.6 and 4.0 Ma (Figure 6). This is in agreement with the earlier studies of outcrops on land indicating glacial retreat with the same age range [Pickard *et al.*, 1988; McMinn and Harwood, 1995]. Although it is also possible that a lack of IRD indicates ice sheet stability with reduced calving rates, such a scenario is unlikely given the recognition of several episodes of sea surface temperatures higher than 2–5°C indicated by the presence of abundant *Dictyochoa* [Bohaty and Harwood, 1998; Whitehead and Bohaty, 2003; Escutia *et al.*, 2009]. Given that current average water temperatures below the Amery Ice Shelf are only –10°C [Fricker *et al.*, 2001] it is likely that during the warm early Pliocene surface temperatures exceeded the stability threshold for ice shelves, which is at mean annual surface temperatures of –5 to –9°C [Cook *et al.*, 2005]. Moreover, the kaolinite content of the sediments is low and there are no stratified beds indicating direct supply of sediment by downslope currents from an ice sheet positioned at the shelf break at any time between 4.6 and 4.0 Ma, not even during glacials. During this time, the western Ross Sea was also free of ice as indicated by presence of a thick diatomite in AND-1B, although an unconformity is present within it spanning 4.3 to 3.6 Ma [Naish *et al.*, 2009].

4.1. Mid-Pliocene Ice Dynamics

[28] The mid-Pliocene (3.3–3.0 Ma) is characterized by glacials with composite benthic oxygen isotope values approaching modern values and superinterglacials with values similar to those of the early Pliocene [Lisiecki and Raymo, 2005], with higher global sea surface temperatures than present [Dowsett *et al.*, 1996], increased melting of marine termini and reduced sea ice conditions [Whitehead *et al.*, 2005]. At 3.55 Ma in Site 1165, IRD MAR displays a brief maximum coinciding with an abrupt increase in terrigenous clay (Figure 6), and a general decrease in sea surface temperatures in the Southern Ocean [Bohaty and Harwood, 1998; Whitehead and Bohaty, 2003]. The provenance of the IRD is primarily from the Lambert drainage basin, but with a significant contribution from the Wilkes Land as well [Williams *et al.*, 2010], consistent with a northerly position of the ACC. A decrease in sea surface temperatures, faster ice flow, and ice advance, therefore, likely contributed to this increase in IRD MAR.

[29] Further, a tenfold increase in IRD MAR at ~3.3 Ma (Figure 6) is apparent, which coincides exactly with the appearance of the M2 glacial in the composite benthic oxygen isotope record [Lisiecki and Raymo, 2005]. The M2 glacial is the first significantly heavy isotope stage after the early Pliocene warm period. The abrupt increase in IRD MAR is most likely caused by the onset of the production of clusters of icebergs from a periodically calving glacier or ice shelf on the continental shelf adjacent to the drill site. Although the increase in IRD MAR may be attributed to faster ice flow, convergent currents near Site 1165, and a decrease in sea surface temperatures, all of these require a glacial advance. Moreover, the presence of plumites or muddy turbidites directly below IRD MAR peaks, suggests that ice advanced to the shelf break prior to occurrence of the peak IRD MAR.

[30] Interpretations of boreholes and seismic data suggest that the Prydz Channel was excavated at around ~3 Ma

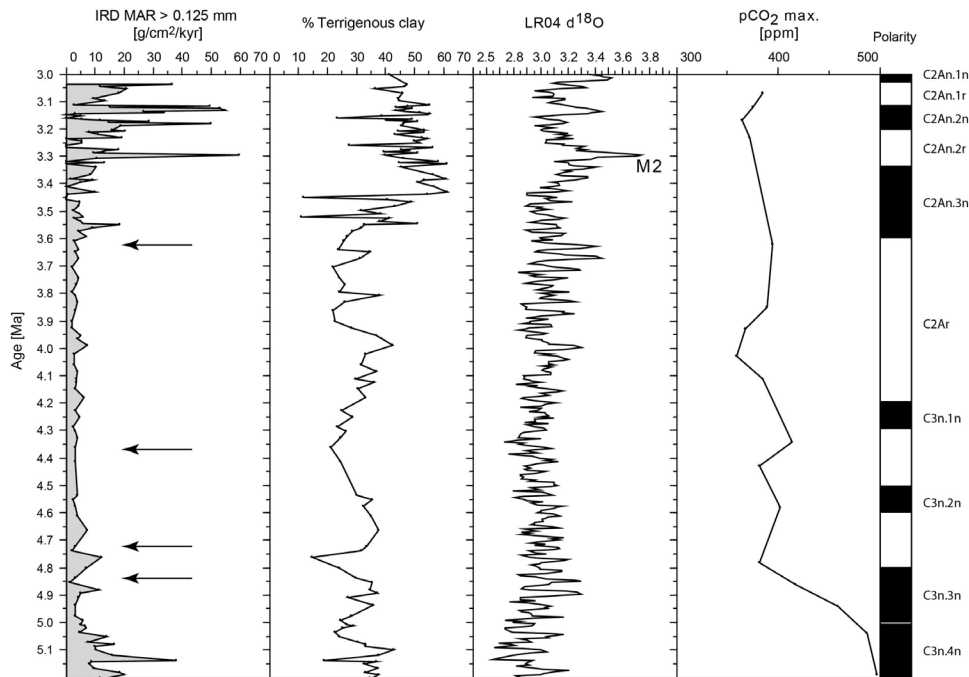


Figure 6. Age distribution of ice rafted debris mass accumulation rates (IRD MAR), terrigenous clay percentage, LR04 stack of oxygen isotope values in benthic foraminifera [Lisiecki and Raymo, 2005], and alkenone-based pCO₂ estimates size corrected with $b = 108$ [Seki et al., 2010]. Arrows indicate positions of intervals recording sea surface temperatures 4–5.5°C higher than present [Whitehead and Bohaty, 2003; Escutia et al., 2009]. Age tie points are listed in Table 1.

[Volpi et al., 2009] coincident with the onset of debris flow activity on the Prydz Channel Fan [Rebesco et al., 2006]. The orientation of the Prydz Channel and the geometry of the trough mouth fan suggest that these advances require an increase in ice drainage from the Ingrid Christensen Coast to the southeast of Prydz Bay [O'Brien et al., 2007]. The sediments associated with the IRD MAR peaks at Site 1165 show local increases in smectite content, which coincide with increases in kaolinite content (Figure 5) [Junttila et al., 2005]. A major unconformity is present between kaolinite and smectite-rich Upper Eocene strata at Site 1166 and 742 on the Prydz continental shelf and illite-rich late Pliocene tills [Hambrey et al., 1991; Forsberg et al., 2008]. I therefore attribute the relative smectite and kaolinite enrichment to glacial erosion of kaolinite and smectite-rich upper Eocene strata on the Prydz Bay continental shelf. These results suggest that the mid-Pliocene IRD MAR peaks are associated with several 100s of km of grounding line advance of the EAIS beyond its present position onto the Prydz Bay continental shelf.

[31] Due to relatively high sedimentation rates, lack of scouring, and excellent age control with 4 age tie points (Table 1) from the bio-magnetostratigraphy in the mid-Pliocene core interval at Site 1165, it is possible to record some orbital scale ice rafting events (Figure 7). A direct correlation between IRD MAR and oxygen isotope excursions in the global benthic isotope stack of Lisiecki and Raymo [2005] is apparent in the mid-Pliocene. Peak intervals of heavier isotope signatures correlate to episodes of peak IRD MAR. The good correlation between IRD MAR at Site 1165 and the globally averaged $\delta^{18}O$ signal suggests that

global ice volume and/or deep-water temperatures may have been physically linked with East Antarctic ice dynamics.

[32] Although small uncertainties in the age model need to be taken into account with these correlations, the peaks of the ice-rafting at Site 1165 tend to occur near the peak glacials of the oxygen isotope record. As discussed above, interlaminated silt and clay intervals directly below IRD MAR maxima represent deposition from ice at the shelf break, suggesting that the IRD peaks signal the onset of the retreat with ice grounded on the shelf. Such a pattern of ice-rafting could indicate the collapse of a marine-grounded ice sheet in response to warming at the onset of the interglacials.

[33] The IRD MAR displays considerable fluctuations between glacials and interglacials and paleontological evidence previously indicated that during interglacials mid-Pliocene sea surface temperatures were periodically higher with reduced sea ice cover [Whitehead et al., 2005]. Further, evidence of periodic glacial retreat of at least several 100s of km is provided by outcrops of mid-Pliocene open marine diatomaceous mudstones in the Lambert Graben rift flank [Whitehead et al., 2004; Passchier and Whitehead, 2006]. Such a contrast in sedimentation between glacials and interglacials requires considerable variations in ice extent and paleoenvironmental conditions, suggesting that the Lambert Glacier-Amery Ice Shelf could have been a dynamic system during this previous episode of warmer climates. In Prydz Bay extreme advances reached the shelf edge at 67°S latitude. Enhanced basal sliding, thinning, and surface melt, could have resulted in ice lift-off and rapid retreat of the grounding line. Further, the landward overdeepening of the Lambert Graben possibly created unstable conditions during glacial

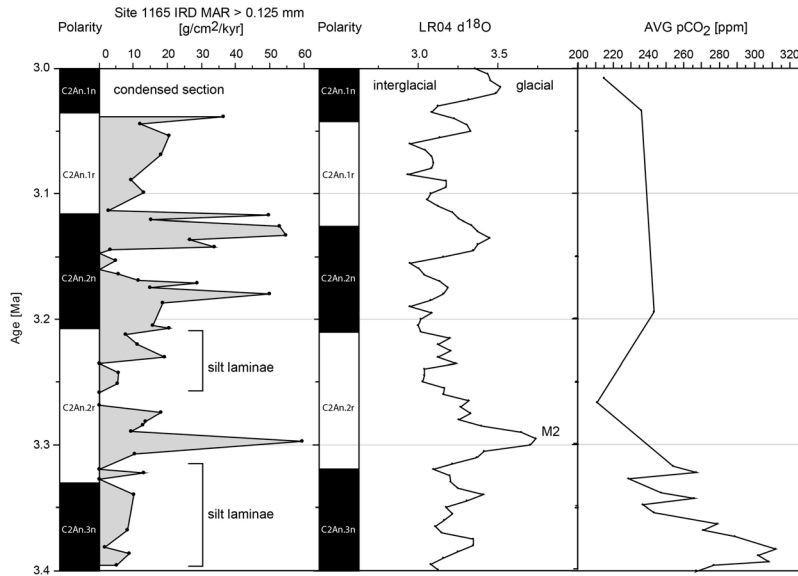


Figure 7. Correlation of mid-Pliocene ice rafted debris mass accumulation rates (IRD MAR), the LR04 stack of oxygen isotope values in benthic foraminifera [Lisiecki and Raymo, 2005], and pCO₂ based on boron/calcium ratios in foraminifera [Tripathi et al., 2009]. The LR04 stack uses slightly different ages for the magnetic reversals than listed in Table 1, differing between 3 and 13 kyr [Lisiecki and Raymo, 2005].

retreat due to decoupling of the ice from its bed once the retreat had been initiated.

4.2. East Antarctic Ice Dynamics, Paleoclimate, and pCO₂

[34] The short-term stability of marine ice sheets in the present period of warming appears to be controlled by surface melt and ocean warming beneath floating margins [Rignot and Jacobs, 2002; Cook et al., 2005; Jenkins et al., 2010]. Global temperatures in the early Pliocene were an estimated 4°C warmer than today, and poor stratification and increased oceanic and/or atmospheric meridional heat transport may have decreased latitudinal temperature gradients, with increased polar warming [Brierley et al., 2009; Ballantyne et al., 2010] and possible implications for marine-based ice. Stable isotope data suggest that relatively strong thermohaline overturn may have contributed to the onset of early Pliocene warmth [Billups, 2002] and that the flux of Northern Component Deep Water (NCDW) was comparable to today's flux in the early Pliocene [Billups et al., 1998]. In response to the high-latitude warming, a southward migration of the ACC may have resulted in enhanced upwelling, which in turn might have caused more inflow of relatively warm NCDW [Hillenbrand and Ehrmann, 2005]. The Lambert Glacier system could have been exceptionally sensitive to ocean warming due to its northerly position and the presence of the overdeepened Lambert Graben. Retreat induced by ocean warming would explain the low IRD MAR between 4.6 and 4.0 Ma at Site 1165 during the early Pliocene warm period.

[35] Cooling and ice growth between ~3.5 and 3.3 Ma is well documented in Antarctica and the Southern Ocean, and the M2 glacial (~3.3 Ma) has an Antarctic-wide significance. Upon termination of the early Pliocene warm period,

the WAIS grounding line advanced across the western Ross Sea following deposition of a thick diatomite interval [Naish et al., 2009]. The advance corresponds to an increase in modeled Antarctic ice volume, including an East Antarctic component, equivalent to an 8-m eustatic fall from 7 m above present-day sea level to 1 m below [Naish et al., 2009; Pollard and DeConto, 2009]. The onset of ice growth at ~3.5–3.3 Ma and the mid-Pliocene extreme ice advances in Prydz Bay may have been a result of increased precipitation and the shifting of major snow accumulation areas in response to changes in atmospheric circulation [O'Brien et al., 2007]. The mechanisms behind these changes are, however, very poorly understood.

[36] On a global scale, modeling studies and paleoclimate records suggest a strong link between pCO₂ and ice dynamics [e.g., DeConto and Pollard, 2003; DeConto et al., 2008; Bintanja and van de Wal, 2008; Tripathi et al., 2009]. A conceptual model proposed by Paillard and Parrenin [2004] suggests that upon Antarctic ice expansion, brine injection from saline shelf waters caused ocean stratification and carbon storage. Boron and alkenone derived reconstructions indicate that the early to mid-Pliocene pCO₂ was higher than pre-industrial values, but the records vary considerably in temporal resolution and absolute values are poorly constrained [Tripathi et al., 2009; Pagani et al., 2010; Seki et al., 2010]. The alkenone-based records of Pagani et al. [2010] and Seki et al. [2010] show variability in the main trends due to low temporal resolution and local environmental influences on the pCO₂ proxies. The reconstructions based on boron/calcium ratios by Tripathi et al. [2009] and Seki et al. [2010] do not cover the warm early Pliocene. All reconstructions seem to show an overall decreasing trend to lower than pre-industrial pCO₂ from the early into the late Pliocene, but the agreement in absolute values and the temporal resolution

is not sufficient to establish lead-lag relationships through correlation with the IRD MAR.

[37] On a regional scale, coupled climate ice sheet models do not predict the extensive dynamics of the Lambert Glacier-Amery Ice Shelf system in the mid-Pliocene as indicated by the record from Site 1165 [Pollard and DeConto, 2009]. Although some models predict surface melt across portions of the EAIS for the mid-Pliocene [Hill et al., 2007], the Lambert Glacier drainage system does not appear to be affected by surface melt nor ocean warming and floating glacial ice of significant thickness is predicted to be present in Prydz Bay even during Pliocene interglacials [Pollard and DeConto, 2009]. The ocean component in the models, however, is relatively crude and the exact mechanisms of poleward heat transfer are poorly understood for the Pliocene permanent El Niño state [Brierley et al., 2009]. The discrepancies in ice extent between models and data can be explained by uncertainties in the dynamical responses of shelf-grounded termini, surface melt, ocean heat uptake and poleward oceanic heat transport.

5. Conclusions

[38] The IRD MAR at Site 1165 is the first well-dated high resolution record documenting the role of EAIS dynamics in the Pliocene warming events. Persistent low IRD MAR at 4.6–4.0 Ma suggest that the Amery Ice Shelf may have been absent and the Lambert Glacier retreated during the early Pliocene warm period under conditions of elevated high-latitude surface temperatures [Ballantyne et al., 2010]. These results are significant, because the Amery Ice Shelf is the largest in East Antarctica and it buttresses the Lambert Glacier system, which drains approximately 14% of the current EAIS. Southern Ocean cooling began at 3.6–3.3 Ma [Whitehead and Bohaty, 2003] with ice advance in the Lambert Glacier system at 3.5 Ma and the onset of extreme advances at 3.3 Ma as recorded in the IRD MAR at Site 1165.

[39] A mid-Pliocene record (3.3–3.0 Ma) at orbital resolution indicates a strong coupling between East Antarctic ice dynamics and the stacked benthic oxygen isotope record [Lisiecki and Raymo, 2005]. The strong coupling suggests that changes in global ice volume and deep-sea temperatures were occurring coincident with East Antarctic ice dynamics. Periodic disintegration of the marine terminus of the Lambert Glacier, as indicated by the IRD MAR at Site 1165, was followed by some ice loss of the EAIS and a retreat of its margin from the marine environment during mid-Pliocene interglacials. Likely mechanisms for the disintegration of the marine terminus are thinning due to basal sliding, surface melt, lift-off and excess basal melting due to the incursion of warmer ocean currents, and accelerated glacial retreat within the overdeepened Lambert Graben. In order to separate local from regional signals, further studies of cores from IODP Exp. 318 will be carried out to collect similar records for another portion of the East Antarctic margin [Expedition 318 Scientists, 2010].

[40] **Acknowledgments.** This research used samples and data provided by the Ocean Drilling Program, which was sponsored by the U.S. National Science Foundation and participating countries under the management of Joint Oceanographic Institutions, Incorporated. This paper is

dedicated to Dietz Warnke who carried out many studies of ice rafted debris in the Southern Ocean and led the effort to obtain Pliocene and Pleistocene high resolution records from Site 1165. His comments on an earlier version of this paper are highly appreciated. I would also like to thank the crew and staff of the JOIDES Resolution and the other members of the Leg 188 Shipboard Scientific Party for valuable discussions and Claus-Dieter Hillenbrand and Tim Naish for excellent reviews that improved this paper. This is a contribution to the SCAR research program Antarctic Climate Evolution (ACE).

References

- Allen, C. P., and D. A. Warnke (1991), History of ice rafting at Leg 114 sites, Subantarctic/South Atlantic, *Proc. Ocean Drill. Program Sci. Results*, *114*, 599–607.
- Ashworth, A. C., and F. C. Thompson (2003), Paleontology: A fly in the biogeographic ointment, *Nature*, *423*, 135–136, doi:10.1038/423135a.
- Baldauf, J. G., and J. A. Barron (1991), Diatom biostratigraphy: Kerguelen Plateau and Prydz Bay regions of the Southern Ocean, *Proc. Ocean Drill. Program, Sci. Results*, *119*, 547–588.
- Ballantyne, A. P., D. R. Greenwood, J. S. Sinninghe Damsté, A. Z. Csank, J. J. Eberle, and N. Rybczynski (2010), Significantly warmer Arctic surface temperatures during the Pliocene indicated by multiple independent proxies, *Geology*, *38*, 603–606, doi:10.1130/G30815.1.
- Bamber, J. L., D. G. Vaughan, and I. Joughin (2000), Widespread complex flow in the interior of the Antarctic Ice Sheet, *Science*, *287*, 1248–1250, doi:10.1126/science.287.5456.1248.
- Bart, P. (2001), Did the Antarctic Ice Sheets expand during the early Pliocene?, *Geology*, *29*, 67–70, doi:10.1130/0091-7613(2001)029<0067:DTAISE>2.0.CO;2.
- Billups, K. (2002), Late Miocene through early Pliocene deep water circulation and climate change viewed from the subantarctic Southern Ocean, *Palaeogeogr. Palaeoclimatol. Palaeoecol.*, *185*, 287–307, doi:10.1016/S0031-0182(02)00340-1.
- Billups, K., A. C. Ravelo, and J. C. Zachos (1998), Early Pliocene deep water circulation in the western equatorial Atlantic: Implications for high-latitude climate change, *Paleoceanography*, *13*(1), 84–95, doi:10.1029/97PA02995.
- Bindoff, N. L., M. A. Rosenberg, and M. J. Warner (2000), On the circulation and water masses over the Antarctic continental slope and rise between 80 and 150°E, *Deep Sea Res., Part II*, *47*, 2299–2326, doi:10.1016/S0967-0645(00)00038-2.
- Bintanja, R., and R. S. W. van de Wal (2008), North American ice-sheet dynamics and the onset of 100,000-year glacial cycles, *Nature*, *454*, 869–872, doi:10.1038/nature07158.
- Bohaty, S. M., and D. M. Harwood (1998), Southern Ocean Pliocene paleotemperature variation from high-resolution silicoflagellate biostratigraphy, *Mar. Micropaleontol.*, *33*, 241–272, doi:10.1016/S0377-8398(97)00037-6.
- Breza, J. R. (1992), High-resolution study of Neogene ice-rafted debris, Site 751, southern Kerguelen Plateau, *Proc. Ocean Drill. Program Sci. Results*, *120*, 207–221.
- Brierley, C. M., A. V. Fedorov, Z. Liu, T. D. Herbert, K. T. Lawrence, and J. P. LaRiviere (2009), Greatly expanded tropical warm pool and weakened Hadley circulation in the early Pliocene, *Science*, *323*, 1714–1718, doi:10.1126/science.1167625.
- Burckle, L. H., A. P. Stroeven, C. Brongre, U. Miller, and A. Wasell (1996), Deficiencies in the diatom evidence for a Pliocene reduction of the East Antarctic Ice Sheet, *Paleoceanography*, *11*(4), 379–389, doi:10.1029/96PA01126.
- Ciesielski, P. F., and F. M. Weaver (1974), Early Pliocene temperature changes in the Antarctic seas, *Geology*, *2*, 511–515, doi:10.1130/0091-7613(1974)2<511:EPTCIT>2.0.CO;2.
- Cook, A. J., A. J. Fox, D. G. Vaughan, and J. G. Ferrigno (2005), Retreating glacier fronts on the Antarctic Peninsula over the past half-century, *Science*, *308*, 541–544, doi:10.1126/science.1104235.
- Cowan, E. A., C.-D. Hillenbrand, L. E. Hassler, and M. T. Ake (2008), Coarse-grained terrigenous sediment deposition on continental rise drifts: A record of Plio-Pleistocene glaciation on the Antarctic Peninsula, *Palaeogeogr. Palaeoclimatol. Palaeoecol.*, *265*, 275–291, doi:10.1016/j.palaeo.2008.03.010.
- Death, R., M. J. Siegert, G. Bigg, and M. Wadley (2006), Modeling Eurasian iceberg meltwater and sedimentation within the North Atlantic at the LGM, *Palaeogeogr. Palaeoclimatol. Palaeoecol.*, *236*, 135–150, doi:10.1016/j.palaeo.2005.11.040.
- DeConto, R., D. Pollard, and D. Harwood (2007), Sea ice feedback and Cenozoic evolution of Antarctic climate and ice sheets, *Paleoceanography*, *22*, PA3214, doi:10.1029/2006PA001350.

- DeConto, R. M., and D. Pollard (2003), Rapid Cenozoic glaciation of Antarctica induced by declining atmospheric CO₂, *Nature*, *421*, 245–249, doi:10.1038/nature01290.
- DeConto, R. M., D. Pollard, P. Wilson, H. Pälike, C. Lear, and M. Pagani (2008), Thresholds for Cenozoic bipolar glaciation, *Nature*, *455*, 652–656, doi:10.1038/nature07337.
- Domack, E. W., and P. Harris (1998), A new depositional model for ice shelves based upon sediment cores from the Ross Sea and the Mac. Robertson shelf, Antarctica, *Ann. Glaciol.*, *27*, 281–284.
- Dowdeswell, J. A., A. Elverhøi, and R. Spielhagen (1998), Glacimarine sedimentary processes and facies on the polar North Atlantic margins, *Quat. Sci. Rev.*, *17*, 243–272, doi:10.1016/S0277-3791(97)00071-1.
- Dowsett, H. J., and T. M. Cronin (1990), High eustatic sea level during the Middle Pliocene: Evidence from the southeastern U.S. Atlantic Coastal Plain, *Geology*, *18*, 435–438, doi:10.1130/0091-7613(1990)018<0435: HESLDT>2.3.CO;2.
- Dowsett, H. J., J. Barron, and R. Poore (1996), Middle Pliocene sea surface temperatures: A global reconstruction, *Mar. Micropaleontol.*, *27*, 13–25, doi:10.1016/0377-8398(95)00050-X.
- Ehrmann, W., and H. Grobe (1991), Cyclic sedimentation at sites 745 and 746, *Proc. Ocean Drill. Program Sci. Results*, *119*, 225–237, doi:10.2973/odp.proc.sr.119.123.1991.
- Ehrmann, W., J. Bloemendal, M. J. Hambrey, B. McKelvey, and J. Whitehead (2003), Variations in the composition of the clay fraction of the Cenozoic Pagodroma Group: Implications for determining provenance, *Sediment. Geol.*, *161*, 131–152, doi:10.1016/S0037-0738(03)00069-1.
- Escutia, C., M. A. Bárcena, R. G. Lucchi, O. Romero, A. M. Ballegeer, J. J. Gonzalez, and D. M. Harwood (2009), Circum-Antarctic warming events between 4 and 3.5 Ma recorded in marine sediments from the Prydz Bay (ODP Leg 188) and the Antarctic Peninsula (ODP Leg 178) margins, *Global Planet. Change*, *69*, 170–184, doi:10.1016/j.gloplacha.2009.09.003.
- Evans, J., and C. J. Pudsey (2002), Sedimentation associated with Antarctic Peninsula ice shelves: Implications for palaeoenvironmental reconstructions of glacial marine sediments, *J. Geol. Soc. London*, *159*(3), 233–237, doi:10.1144/0016-764901-125.
- Expedition 318 Scientists (2010), Wilkes Land glacial history: Cenozoic East Antarctic Ice Sheet evolution from Wilkes Land margin sediments, *Integr. Ocean Drill. Program Prelim. Rep.*, *318*, doi:10.2204/iudp.pr.318.2010.
- Florindo, F., S. M. Bohaty, P. S. Erwin, C. Richter, A. P. Roberts, P. A. Whalen, and J. M. Whitehead (2003), Magnetobiostratigraphic chronology and palaeoenvironmental history of Cenozoic sequences from ODP Sites 1165 and 1166, Prydz Bay, Antarctica, *Palaeogeogr. Palaeoclimatol. Palaeoecol.*, *198*, 69–100, doi:10.1016/S0031-0182(03)00395-X.
- Folk, R. L., and W. C. Ward (1957), Brazos River bar: A study in the significance of grain size parameters, *J. Sediment. Petrol.*, *27*, 3–26.
- Forsberg, C. F., F. Florindo, J. Gruetzner, A. Venuti, and A. Solheim (2008), Sedimentation and aspects of glacial dynamics from physical properties, mineralogy and magnetic properties at ODP Sites 1166 and 1167, Prydz Bay, Antarctica, *Palaeogeogr. Palaeoclimatol. Palaeoecol.*, *260*, 184–201, doi:10.1016/j.palaeo.2007.08.022.
- Fricker, H. A., S. Popov, I. Allison, and N. Young (2001), Distribution of marine ice beneath the Amery Ice Shelf, *Geophys. Res. Lett.*, *28*(11), 2241–2244, doi:10.1029/2000GL012461.
- Fricker, H. A., R. Coleman, L. Padman, T. A. Scambos, J. Bohlander, and K. M. Brunt (2009), Mapping the grounding zone of the Amery Ice Shelf, East Antarctica using InSAR, MODIS and ICESat, *Antarct. Sci.*, *21*, 515–532, doi:10.1017/S095410200999023X.
- Gersonde, R., et al. (1997), Geological record and reconstruction of the late Pliocene impact of the Eltanin asteroid in the Southern Ocean, *Nature*, *390*, 357–363, doi:10.1038/37044.
- Gradstein, F., J. Ogg, and A. Smith (Eds.) (2004), *A Geologic Time Scale 2004*, 589 pp., Cambridge Univ. Press, Cambridge, U. K.
- Grützner, J., C.-D. Hillenbrand, and M. Rebesco (2005), Terrigenous flux and biogenic silica deposition at the Antarctic continental rise during the late Miocene to early Pliocene: Implications for ice sheet stability and sea ice coverage, *Global Planet. Change*, *45*, 131–149, doi:10.1016/j.gloplacha.2004.09.004.
- Hambrey, M. J., and B. McKelvey (2000), Major Neogene fluctuations of the East Antarctic ice sheet: Stratigraphic evidence from the Lambert Glacier region, *Geology*, *28*, 887–960, doi:10.1130/0091-7613(2000)28<887: MNFOTE>2.0.CO;2.
- Hambrey, M. J., W. U. Ehrmann, and B. Larsen (1991), Cenozoic glacial record of the Prydz Bay continental shelf, East Antarctica, *Proc. Ocean Drill. Program Sci. Results*, *119*, 77–132.
- Hambrey, M. J., M. R. Bennett, J. A. Dowdeswell, N. F. Glasser, and D. Huddard (1999), Debris entrainment and transfer in polythermal valley glaciers, *J. Glaciol.*, *149*(45), 69–86.
- Harwood, D. M. (1986), Diatom biostratigraphy and paleoecology with a Cenozoic history of Antarctic ice sheets, Ph.D. thesis, Ohio State Univ., Columbus.
- Harwood, D. M., and P.-N. Webb (1998), Glacial transport of diatoms in the Antarctic Sirius Group: Pliocene refrigerator, *GSA Today*, *8*(4), 1–8.
- Haug, G. H., R. Tiedemann, R. Zahn, and A. C. Ravelo (2001), Role of Panama uplift on oceanic freshwater balance, *Geology*, *29*, 207–210, doi:10.1130/0091-7613(2001)029<0207:ROPUOO>2.0.CO;2.
- Haywood, A. M., et al. (2009a), Middle Miocene to Pliocene history of Antarctica and the Southern Ocean, in *Antarctic Climate Evolution*, *Dev. Earth Environ. Sci.*, vol. 8, edited by F. Florindo and M. Sievert, pp. 401–463, Elsevier, Amsterdam, Netherlands.
- Haywood, A. M., H. J. Dowsett, P. J. Valdes, D. J. Lunt, J. E. Francis, and B. W. Sellwood (2009b), Introduction. Pliocene climate, processes and problems, *Philos. Trans. R. Soc. A*, *367*, 3–17, doi:10.1098/rsta.2008.0205.
- Hesse, R., S. Khodabakhsh, I. Klauke, and W. B. F. Ryan (1997), Asymmetrical turbid surface-plume deposition near ice-outlets of the Pleistocene Laurentide ice sheet in the Labrador Sea, *Geo Mar. Lett.*, *17*, 179–187, doi:10.1007/s003670050024.
- Hill, D. J., A. M. Haywood, R. C. A. Hindmarsh, and P. J. Valdes (2007), Characterising ice sheets during the mid-Pliocene: Evidence from data and models, in *Deep-Time Perspectives on Climate Change: Marrying the Signal From Computer Models and Biological Proxies*, edited by M. Williams et al., pp. 517–538, Geol. Soc., London.
- Hillenbrand, C.-D., and W. Ehrmann (2005), Late Neogene to Quaternary environmental changes in the Antarctic Peninsula region: Evidence from drift sediments, *Global Planet. Change*, *45*, 165–191, doi:10.1016/j.gloplacha.2004.09.006.
- Hönisch, B., N. G. Hemming, D. Archer, M. Siddall, and J. F. McManus (2009), Atmospheric carbon dioxide concentration across the Mid-Pleistocene transition, *Science*, *324*, 1551–1554, doi:10.1126/science.1171477.
- Hosie, G. W., and T. G. Cochran (1994), Mesoscale distribution patterns of macrozooplankton communities in Prydz Bay, Antarctica - January to February 1991, *Mar. Ecol. Prog. Ser.*, *106*, 21–39, doi:10.3354/mei106021.
- Hultsch, N., B. Wagner, B. Diekmann, and D. White (2008), Mineralogical implications for the Late Pleistocene glaciation in Amery Oasis, East Antarctica, from a lake sediment core, *Antarct. Sci.*, *20*, 169–172, doi:10.1017/S0954102007000880.
- Jansen, E., et al. (2007), Palaeoclimate, in *Climate Change 2007: The Physical Science Basis: Contribution of Working Group I to the Fourth Assessment Report of the Intergovernmental Panel on Climate Change*, edited by S. Solomon et al., pp. 433–497, Cambridge Univ. Press, New York.
- Jenkins, A., P. Dutrieux, S. S. Jacobs, S. D. McPhail, J. R. Perrett, A. T. Webb, and D. White (2010), Observations beneath Pine Island Glacier in West Antarctica and implications for its retreat, *Nat. Geosci.*, *3*, 468–472, doi:10.1038/ngeo890.
- Joseph, L. H., D. K. Rea, B. A. van der Pluijm, and J. D. Gleason (2002), Antarctic environmental variability since the late Miocene: ODP Site 745, the East Kerguelen sediment drift, *Earth Planet. Sci. Lett.*, *201*, 127–142, doi:10.1016/S0012-821X(02)00661-1.
- Junttila, J., M. Ruikka, and K. Strand (2005), Clay-mineral assemblages in high-resolution Plio-Pleistocene interval at ODP Site 1165, Prydz Bay, Antarctica, *Global Planet. Change*, *45*, 151–163, doi:10.1016/j.gloplacha.2004.09.007.
- Konert, M., and J. Vandenberghe (1997), Comparison of laser grain size analysis with pipette and sieve analysis: A solution for the underestimation of the clay fraction, *Sedimentology*, *44*, 523–535, doi:10.1046/j.1365-3091.1997.d01-38.x.
- Krantz, D. E. (1991), A chronology of Pliocene sea-level fluctuations: The US Middle Atlantic Coastal Plain record, *Quat. Sci. Rev.*, *10*, 163–174, doi:10.1016/0277-3791(91)90016-N.
- Krissek, L. A. (1995), Late Cenozoic ice-rafting records from Leg 145 sites in the North Pacific: Late Miocene onset, late Pliocene intensification, and Pliocene-Pleistocene events, *Proc. Ocean Drill. Program Sci. Results*, *145*, 179–194.
- Lekens, W., H. P. Sejrup, H. Hafliadason, G. O. Petersen, B. Hjelstuen, and G. Knorr (2005), Laminated sediments preceding Heinrich event 1 in the northern North Sea and southern Norwegian Sea: Origin, processes and regional linkage, *Mar. Geol.*, *216*, 27–50, doi:10.1016/j.margeo.2004.12.007.
- Lisiecki, L. E., and M. E. Raymo (2005), A Pliocene-Pleistocene stack of 57 globally distributed benthic $\delta^{18}O$ records, *Paleoceanography*, *20*, PA1003, doi:10.1029/2004PA001071.
- Lucchi, R. G., M. Rebesco, A. Camerlenghi, M. Busetti, L. Tomadin, G. Villa, D. Persico, C. Morigi, M. C. Bonci, and G. Giorgetti (2002),

- Glacimarine sedimentary processes of a high-latitude, deep-sea sediment drift (Antarctic Peninsula Pacific margin), *Mar. Geol.*, 189, 343–370, doi:10.1016/S0025-3227(02)00470-X.
- Lythe, M. B., D. G. Vaughan, and BEDMAP Consortium (2001), BEDMAP: A new ice thickness and subglacial topographic model of Antarctica, *J. Geophys. Res.*, 106, 11,335–11,351, doi:10.1029/2000JB900449.
- Marchant, D. R., G. H. Denton, D. E. Sugden, and C. C. Swisher III (1993), Miocene glacial stratigraphy and landscape evolution of the western Asgard Range, Antarctica, *Geogr. Ann., Ser. A*, 75(4), 303–330.
- McMinn, A., and D. Harwood (1995), Biostratigraphy and palaeoecology of early Pliocene diatom assemblages from the Larsemann Hills, eastern Antarctica, *Antarct. Sci.*, 7, 115–116, doi:10.1017/S0954102095000149.
- Miller, K. G., M. A. Komiz, J. V. Browning, J. D. Wright, G. S. Mountain, M. E. Katz, P. J. Sugarman, B. S. Cramer, N. Christie-Blick, and S. F. Pekar (2005), The Phanerozoic record of global sea-level change, *Science*, 310, 1293–1298, doi:10.1126/science.1116412.
- Murphy, L., D. A. Warnke, C. Andersson, J. Channell, and J. Stoner (2002), History of ice rafting at South Atlantic ODP Site 177-1092 during the Gauss and Late Gilbert Chrons, *Palaeogeogr. Palaeoclimatol. Palaeoecol.*, 182, 183–196, doi:10.1016/S0031-0182(01)00495-3.
- Naish, T. R., and G. Wilson (2009), Constraints on the amplitude of Mid-Pliocene (3.6–2.4 Ma) eustatic sea-level fluctuations from the New Zealand shallow-marine sediment record, *Philos. Trans. R. Soc. A*, 367, 169–187, doi:10.1098/rsta.2008.0223.
- Naish, T., et al. (2009), Obliquity-paced Pliocene West Antarctic Ice Sheet oscillations, *Nature*, 458, 322–328, doi:10.1038/nature07867.
- O'Brien, P. E., I. Goodwin, C.-F. Forsberg, A. K. Cooper, and J. Whitehead (2007), Late Neogene ice drainage changes in Prydz Bay, East Antarctica and the interaction of Antarctic Ice Sheet evolution and climate, *Palaeogeogr. Palaeoclimatol. Palaeoecol.*, 245, 390–410, doi:10.1016/j.palaeo.2006.09.002.
- Ó Cofaigh, C., J. A. Dowdeswell and H. Grobe (2001), Holocene glacimarine sedimentation, inner Scoresby Sund, East Greenland: The influence of fast-flowing ice-sheet outlet glaciers, *Mar. Geol.*, 175, 103–129, doi:10.1016/S0025-3227(01)00117-7.
- Pagani, M., Z. Liu, J. LaRivière, and A. C. Ravelo (2010), High Earth-system climate sensitivity determined from Pliocene carbon dioxide concentrations, *Nat. Geosci.*, 3, 27–30, doi:10.1038/ngeo724.
- Paillard, D., and F. Parrenin (2004), The Antarctic Ice Sheet and the triggering of deglaciations, *Earth Planet. Sci. Lett.*, 227, 263–271, doi:10.1016/j.epsl.2004.08.023.
- Passchier, S., and J. M. Whitehead (2006), Anomalous geochemical provenance and weathering history of Plio-Pleistocene glaciomarine fjord strata, Bardin Bluffs Formation, East Antarctica, *Sedimentology*, 53, 929–942, doi:10.1111/j.1365-3091.2006.00796.x.
- Passchier, S., P. E. O'Brien, J. E. Damuth, N. Januszczak, D. A. Handwerker, and J. M. Whitehead (2003), Pliocene-Pleistocene glaciomarine sedimentation in eastern Prydz Bay and development of the Prydz trough-mouth fan, ODP Sites 1166 and 1167, East Antarctica, *Mar. Geol.*, 199, 279–305, doi:10.1016/S0025-3227(03)00160-9.
- Pickard, J., D. A. Adamson, D. M. Harwood, G. H. Miller, P. G. Quilty, and R. K. Dell (1988), Early Pliocene marine sediments, coastline, and climate of East Antarctica, *Geology*, 16, 158–161, doi:10.1130/0091-7613(1988)016<0158:EPMSCA>2.3.CO;2.
- Pollard, D., and R. M. DeConto (2009), Modelling West Antarctic Ice Sheet growth and collapse through the past five million years, *Nature*, 458, 329–332, doi:10.1038/nature07809.
- Powell, R. D., and B. F. Molnia (1989), Glacimarine sedimentary processes, facies and morphology of the south-southeast Alaska shelf and fjords, *Mar. Geol.*, 85, 359–390, doi:10.1016/0025-3227(89)90160-6.
- Pritchard, H. D., and D. G. Vaughan (2007), Widespread acceleration of tidewater glaciers on the Antarctic Peninsula, *J. Geophys. Res.*, 112, F03S29, doi:10.1029/2006JF000597.
- Pritchard, H. D., R. J. Arthern, D. G. Vaughan, and L. A. Edwards (2009), Extensive dynamic thinning on the margins of the Greenland and Antarctic ice sheets, *Nature*, 461, 971–975, doi:10.1038/nature08471.
- Pudsey, C. J. (1991), Grain size and diatom content of hemipelagic sediments at Site 697, ODP Leg 113: A record of Pliocene-Pleistocene climate, *Proc. Ocean Drill. Program Sci. Results*, 113, 111–120.
- Pudsey, C. J. (2000), Sedimentation on the continental rise west of the Antarctic Peninsula over the last three glacial cycles, *Mar. Geol.*, 167, 313–338, doi:10.1016/S0025-3227(00)00039-6.
- Rebesco, M. (2003), Data report: Numerical evaluation of diffuse spectral reflectance data and correlation with core photos, ODP Site 1165, Wild Drift, Cooperation Sea, Antarctica, *Proc. Ocean Drill. Program Sci. Results*, 188, 1–27, doi:10.2973/odp.proc.sr.188.006.2003.
- Rebesco, M., A. Camerlenghi, R. Getletti, and M. Canals (2006), Margin architecture reveals the transition to the modern Antarctic ice sheet ca. 3 Ma, *Geology*, 34, 301–304, doi:10.1130/G22000.1.
- Rignot, E., and S. S. Jacobs (2002), Rapid bottom melting widespread near Antarctic Ice Sheet grounding lines, *Science*, 296, 2020–2023, doi:10.1126/science.1070942.
- Rignot, E., and R. H. Thomas (2002), Mass balance of polar ice sheets, *Science*, 297, 1502–1506, doi:10.1126/science.1073888.
- Rignot, E., J. Bamber, M. van den Broeke, C. Davis, Y. Li, W. van de Berg, and E. van Meijgaard (2008), Recent mass loss of the Antarctic Ice Sheet from dynamic thinning, *Nat. Geosci.*, doi:10.1038/ngeo102.
- Roy, M., T. van de Flierdt, S. R. Hemming, and S. L. Goldstein (2007), ⁴⁰Ar/³⁹Ar ages of hornblende grains and bulk Sm/Nd isotopes of circum-Antarctic glacio-marine sediments: Implications for sediment provenance in the southern ocean, *Chem. Geol.*, 244(3–4), 507–519, doi:10.1016/j.chemgeo.2007.07.017.
- Seki, O., G. L. Foster, D. N. Schmidt, A. Mackensen, K. Kawamura, and R. D. Pancost (2010), Alkenone and boron based Pliocene pCO₂ records, *Earth Planet. Sci. Lett.*, 292, 201–211, doi:10.1016/j.epsl.2010.01.037.
- Shipboard Scientific Party (2001), Site 1165 [online], *Ocean Drill. Program Initial Rep.*, 188, edited by P. E. O'Brien, A. K. Cooper, and C. Richter, 191 pp., doi:10.2973/odp.proc.ir.188.103.2001. [Available at http://www-odp.tamu.edu/publications/188_IR/VOLUME/CHAPTERS/IR188_03.PDF]
- Sperazza, M., J. N. Moore, and M. Hendrix (2004), High-resolution particle size analysis of naturally occurring very fine-grained sediment through laser diffractometry, *J. Sediment. Res.*, 74(5), 736–743, doi:10.1306/031104740736.
- Steph, S., R. Tiedemann, M. Prange, J. Groeneveld, D. Nürnberg, L. Reuning, M. Schulz, and G. H. Haug (2006), Changes in Caribbean surface hydrography during the Pliocene shoaling of the Central American Seaway, *Paleoceanography*, 21, PA4221, doi:10.1029/2004PA001092.
- Stroeven, A., L. H. Burckle, J. Kleman, and M. L. Prentice (1998), Atmospheric transport of diatoms in the Antarctic Sirius Group: Pliocene Deep Freeze, *GSA Today*, 8(4), 1–5.
- Sugden, D., and G. Denton (2004), Cenozoic landscape evolution of the Convey Range to Mackay Glacier area, Transantarctic Mountains: Onshore to offshore synthesis, *Geol. Soc. Am. Bull.*, 116, 840–857, doi:10.1130/B25356.1.
- Tedford, R. H., and C. R. Harington (2003), An Arctic mammal fauna from the Early Pliocene of North America, *Nature*, 425, 388–390, doi:10.1038/nature01892.
- Thompson, R. S., and R. F. Fleming (1996), Middle Pliocene vegetation: Reconstructions, paleoclimatic inferences, and boundary conditions for climatic modeling, *Mar. Micropaleontol.*, 27, 27–26, doi:10.1016/0377-8398(95)00051-8.
- Tripathi, A. K., C. D. Roberts, and R. A. Eagle (2009), Coupling of CO₂ and ice sheet stability over major climate transitions of the last 20 million years, *Science*, 326, 1394–1397, doi:10.1126/science.1178296.
- Tulaczyk, S., B. Kamb, R. P. Scherer, and H. F. Engelhardt (1998), Sedimentation processes at the base of a West Antarctic ice stream: Constraints from textural and compositional properties of subglacial debris, *J. Sediment. Res.*, 68(3), 487–496.
- Villa, G., C. Lupi, M. Cobianchi, F. Florindo, and S. F. Pekar (2008), A Pleistocene warming event at 1 Ma in Prydz Bay, East Antarctica: Evidence from ODP Site 1165, *Palaeogeogr. Palaeoclimatol. Palaeoecol.*, 260, 230–244, doi:10.1016/j.palaeo.2007.08.017.
- Volpi, V., M. Rebesco, and P. Diviacco (2009), New insights in the evolution of Antarctic glaciation from depth conversion of well-log calibrated seismic section of Prydz Bay, *Int. J. Earth Sci.*, 98(8), 1991–2007, doi:10.1007/s00531-008-0356-6.
- Wara, M. W., A. C. Ravelo, and M. L. Delaney (2005), Permanent El Niño-like conditions during the Pliocene warm period, *Science*, 309, 758–761, doi:10.1126/science.1112596.
- Warnke, D. A., C. P. Allen, D. W. Mueller, D. A. Hodell, and C. Brunner (1992), Miocene-Pliocene Antarctic glacial evolution: A synthesis of ice-rafted debris, stable isotope, and planktonic foraminiferal indicators, ODP Leg 114, in *The Antarctic Paleoenvironment: A Perspective on Global Change*, *Antarct. Res. Ser.*, vol. 56, edited by J. P. Kennett and D. A. Warnke, pp. 311–325, AGU, Washington, D. C.
- Warnke, D. A., C. Richter, F. Florindo, J. E. Damuth, W. L. Balsam, K. Strand, M. Ruiikka, J. Junttila, K. Theissen, and P. Quilty (2004), Data report: HiRISC (High-Resolution Integrated Stratigraphy Committee) Pliocene-Pleistocene interval, 0–50 mbsf, at ODP Leg 188 Site 1165, Prydz Bay, Antarctica [online], *Proc. Ocean Drill. Program Sci. Results*, 188. [Available at http://www-odp.tamu.edu/publications/188_SR/015/015.htm.]
- Whitehead, J. M., and S. M. Bohaty (2003), Pliocene summer sea surface temperature reconstruction using silicoflagellates from Southern Ocean ODP Site 1165, *Paleoceanography*, 18(3), 1075, doi:10.1029/2002PA000829.

- Whitehead, J. M., D. M. Harwood, B. C. McKelvey, M. J. Hambrey, and A. McMinn (2004), Diatom biostratigraphy of the Cenozoic glaciomarine Pagodroma Group, northern Prince Charles Mountains, East Antarctica, *Aust. J. Earth Sci.*, 51(4), 521–547, doi:10.1111/j.1400-0952.2004.01072.x.
- Whitehead, J. M., S. Wotherspoon, and S. M. Bohaty (2005), Minimal Antarctic sea ice during the Pliocene, *Geology*, 33, 137–140, doi:10.1130/G21013.1.
- Whitehead, J. M., W. Ehrmann, D. M. Harwood, C.-D. Hillenbrand, P. G. Quilty, C. Hart, M. Taviani, V. Thorn, and A. McMinn (2006), Late Miocene paleoenvironment of the Lambert Graben embayment, East Antarctica, evident from: Mollusc paleontology, sedimentology and geochemistry, *Global Planet. Change*, 50, 127–147, doi:10.1016/j.gloplacha.2005.07.003.
- Williams, T., T. van de Flierdt, S. R. Hemming, E. Chung, M. Roy, and S. L. Goldstein (2010), Evidence for iceberg armadas from East Antarctica in the Southern Ocean during the late Miocene and early Pliocene, *Earth Planet. Sci. Lett.*, 290, 351–361, doi:10.1016/j.epsl.2009.12.031.
- Young, N. W., D. Turner, G. Hyland, and R. N. Williams (1998), Near-coastal iceberg distributions in East Antarctica, 50–145°E, *Ann. Glaciol.*, 27, 68–74.
- Zwally, H. J., W. Abdalati, T. Herring, K. Larson, J. Saba, and K. Steffen (2002), Surface melt-induced acceleration of Greenland Ice-Sheet flow, *Science*, 297, 218–222, doi:10.1126/science.1072708.

S. Passchier, Department of Earth and Environmental Studies, Montclair State University, Upper Montclair, NJ 07043, USA. (passchiers@mail.montclair.edu)